DOI: 10.1021/ma900541x

Macromolecules
ARTICLE

Re-examination of Dynamics of Polyeletrolytes in Salt-Free Dilute Solutions by Designing and Using a Novel Neutral−Charged−Neutral Reversible Polymer

Kejin Zhou,[†] Junfang Li,[‡] Yijie Lu,[‡] Guangzhao Zhang,[‡] Zuowei Xie,[†,§] and Chi Wu*[,‡,§]

[†]*Shanghai-Hong Kong Joint Laboratory in Chemical Synthesis, Shanghai Institute of Organic Chemistry, Chinese Academy of Sciences, 354 Fenglin Lu, Shanghai 200032, China,* [‡]*The Hefei National Laboratory for Physical Sciences at Microscale, Department of Chemical Physics, University of Science and Technology of China, Hefei, China, and* [§]*Department of Chemistry, The Chinese University of Hong Kong, Shatin, N.T., Hong Kong, China*

Received March 13, 2009; Revised Manuscript Received August 18, 2009

ABSTRACT: By using the Staudinger ligation to attach 4-{5′-[1″-(dimethylamino)-ethylideneamino]pentyl}-1-methyl-2-(diphenylphosphino)terephthalate to poly(*p*-azidomethylstyrene)-*co*-polystyrene (PAMS-*co*-PS), we successfully prepared a novel polymer that can undergo a neutral−charged−neutral transition in DMF with 0.5% H_2O when the solution is alternatively bubbled with CO_2 and N_2. Such a reversible change is confirmed by its sharp conductivity variation. Armed with this polymer, we re-examined dynamics of salt-free polyelectrolyte dilute solutions by using laser light scattering (LLS). As expected, there exists only one diffusive relaxation mode in the neutral state. The bubbling of CO_2 decreases the scattering intensity and splits this initial diffusive relaxation mode into a fast and a slow diffusive mode, and their scattering intensity contributions are independent of the scattering angle, indicating that the slow mode is not related to some scattering objects larger than the LLS observation length ($\sim$35 nm $< 1/q <$ $\sim$190 nm). The bubbling of N_2 gradually diminishes the slow mode and returns both the scattering intensity and solution dynamics back to their initial neutral state. The change from dilute to semidilute solution slows the fast relaxation down and suppresses the slow mode. On the other hand, the addition of LiBr (50 mM) can completely suppress electrostatic interaction.

Introduction

Dynamics of polyeletrolytes in salt-free or low-salt solutions has attracted much attention after Lin et al.[1] reported their dynamic laser light-scattering (LLS) observation of an extremely slow diffusive mode in the low-salt poly(L-lysine) solutions. Later, it was shown that there are actually a fast and a slow relaxation mode in dynamic LLS measurements of salt-free or low-salt dilute polyelectrolyte solutions in comparison with the translational diffusive relaxation mode of individual neutral chains with similar lengths.[2] Some reported slow relaxation modes were really slow with a hydrodynamic size of 10^2-10^3 nm or larger. Gradually, such two modes have been reported for nearly all charged macromolecules, including both synthetic and biological polyelectrolytes with different chain configurations in aqueous and nonaqueous solutions.[2−15] Therefore, these two modes are general features of salt-free or low-salt polyelectrolyte solutions. Generally, such unique dynamics of charged chains in solutions is attributed to intrachain and interchain electrostatic interaction. However, dynamics of polyelectrolyte solutions, especially the slow mode, is still less understood in comparison with that of neutral polymer solutions.[16−18]

The fast mode in polymer dilute and semidilute solutions has been attributed to different origins,[1,4−6,9] such as propagation of excitations in a polyelectrolyte pseudolattice or the free diffusion of the noncaged chains/particles, while the slow mode was related to the hindered center-of-mass diffusion of some caged chains/particles.[8] When polymer chains are charged in a salt-free or low-salt dilute solution, their translational diffusive relaxation mode splits into a fast and a slow diffusive relaxation modes. Lee et al.[17] and Muthukumar[18] suggested that the fast mode, independent of the chain length, would be related to the coupled diffusion (D_f) of polyelectrolyte chains and their small counterions; namely, in a salt-free or low salt solution, the counterions must be condensed nearby the chain backbone, and the fluctuation of these condensed small counterions toward and away from each chain backbone induces an electric field that leads to an electrophoresis-mobility-related diffusive relaxation. Note that small counterions are invisible in LLS when macromolecules exist because of their weak scattering.

On the other hand, the interpretation of the slow mode, especially for those very slow relaxation modes observed in salt-free or low-salt polyelectrolyte solutions, is even more controversial. It has been attributed to or argued for large multichain domains (transient/temporal aggregates or clusters) formed due to electrostatic interaction[7−10] or some insoluble clusters or even a trace amount of large particles introduced during the imperfect preparation of polymer solution.[19−23] The transient-cluster interpretation was supported by studies of poly(*N*-methyl-2-vinylpyridinium chloride) (PMVP) in organic solvents and poly(styrenesulfonate) (NaPSS) with sodium counterions in aqueous solutions under dialysis.[12,24,25]

For a long time, the temporal aggregates have been attributed to the effective interaction between similarly charged segments,[18,26−29] namely, the overlapping of the ion clouds of neighboring polyions so that the more loosely associated small ions are "shared" by two or more polyions chains, resulting in a fluctuating dipole field that tends to retard the relative motions of those participating polyions. It should be noted that the slow mode observed in

*Corresponding author. The Hong Kong address should be used for all correspondence.

 Published on Web 08/28/2009

semidilute neutral polymer solutions is different from what we are discussing here.[30−33] Note that a slowly moving subject which is not necessarily large could be due to some interaction.[33]

Experimentally, a polymer solution is normally prepared by allowing a macroscopic piece of polymer to dissolve in a solvent. The so-called permanent chain clusters must be from the incomplete dissolution in the solution preparation, not the chain association, because we do not place individual chains into a solvent. Revently, Cong et al.[25] detailed those possible problems and prepared a "virgin" NaPSS sample directly from 4-styrenesulfonic sodium salt in an aqueous medium. They then used dialysis to *in situ* change the salt concentration. Even in that case, the solution cleanliness still deteriorated after some dialysis.

Ideally, one would like to have a solution in which polymer chains can be *in situ* switched from a completely neutral to a fully charged state by some chemical reactions under a mild condition. It is worth noting that polymers with some weak acids groups, such as acrylic acid under different pH values, are not good candidates because they are still slightly charged even at a very lower pH. We have searched such a system for a long time. A few years ago, we noted that amidines can readily react with gaseous CO_2 in water or alcohol to form bicarbonate or alkylcarbonate salts, and the reaction is completely reversible if N_2 or Ar is bubbled through the solution.[34,35] This leads us to think that if these amidine motifs could be introduced into polymer chains, we should have an ideal polymer that can be switched between a neutral and a charged state in a solution by alternating bubbling of CO_2 and N_2. In this way, we will rule out any interference of impurities or permanent chains clusters on solution dynamics.

Synthetically, it has been known that TEMPO-mediated living radical copolymerization of styrene and its derivatives can lead to narrowly distributed polymer chains with a controllable length.[36−39] Therefore, we used the following synthetic strategy to prepare such a novel polymer: (1) preparation of narrowly distributed poly(*p*-chloromethylstyrene)-*co*-polystyrene (PCMS-*co*-PS) by using living free-radical reaction; (2) postmodification of PCMS-*co*-PS into poly(*p*-azidomethylstyrene)-*co*-polystyrene (PAMS-*co*-PS); (3) introduction of amidine motifs into PAMS-*co*-PS, after many different failed methods, by using the Staudinger ligation.[40−43] In this way, we have successfully obtained a novel polymer that can undergo a reversible neutral−charged−neutral transition when CO_2 and N_2 are alternatively bubbled through its DMF solution. Armed with this novel polymer, we *in situ* studied the variation of solution dynamics of polymer chains during the neutral−charged−neutral transition.

Experimental Section

Materials and Instruments. Styrene (S) and *p*-chloromethylstyrene (CMS) were purified by vacuum distillation from CaH_2 before use. 2,2,6,6-Tetramethylpiperidine-1-oxyl (TEMPO) (Aldrich) was recrystallized from *n*-hexane prior to use. Methanol (CH_3OH) and dichloromethane (CH_2Cl_2) were distilled over calcium hydride. *N*-(*tert*-Butoxylcarbonyl)aminopentanol[44] and *N*,*N*-dimethylacetamide dimethyl acetal[45] were synthesized according to literature methods. All other reagents were purchased from Aldrich and used as received unless otherwise specified.

^1H, ^{13}C, and ^{31}P NMR spectra were recorded on a Varian Mercury 300 spectrometer at 300.0, 74.5, and 121.0 MHz, respectively. All chemical shifts were reported in δ units with reference to the residual protons of the deuterated solvents for ^1H and ^{13}C chemical shifts and to external H_3PO_4 (80%) for ^{31}P chemical shifts.

Relative molecular weights and molecular weight distributions were determined by one of two gel permeation chromatography (GPC) systems. One is equipped with a Waters 1515 Isocratic HPLC pump, a Waters 2414 refractive index detector (RI), and a set of Waters Styragel columns (HR3, HR4, and HR5, 7.8 × 300 mm). GPC measurements were carried out at 35 °C using THF as eluent with a 1.0 mL/min flow rate. The other is with a Waters 515 Isocratic HPLC pump and a set of Waters Styragel columns (HR1, HR3, and HR4, 7.8 × 300 mm). GPC measurements were done at 60 °C using DMF or DMF containing 50 mM of LiBr as eluent with a 1.0 mL/min flow rate. Both were calibrated with polystyrene standards.

Preparation of 1-Methyl-2-iodoterephthalate (1). The solution of 1-methyl-2-aminoterephthalate (3.00 g, 15.40 mmol) in hydrochloric acid (4 M, 80 mL) was cooled in an ice−salt bath, to which was slowly added an aqueous solution (25 mL) of sodium nitrite (1.17 g, 1.69 mmol) over a period of 0.5 h. The mixture was stirred at this temperature for another 0.5 h. An aqueous solution (100 mL) of potassium iodide (13.00 g, 77.00 mmol) was cooled to −15 °C and then added into the reaction mixture. The mixture was stirred at room temperature for 4 h. After addition of a saturated sodium sulphite aqueous solution (50 mL), the precipitation was collected by filtration and washed with a large amount of water. Recrystallization of this crude product from a methanol/water solution gave **1** as yellow crystals (3.80 g, 81%). ^1H NMR ($CDCl_3$): δ 3.97 (s, 3H), 7.84 (d, J = 8.0 Hz, 1H), 8.12 (dd, J = 1.4 and 8.0 Hz, 1H), 8.69 (d, J = 1.4 Hz, 1H), the same as those in the literature.[42]

Preparation of 1-Methyl-2-(diphenylphosphino)terephthalate (2). To a dry methanol (15 mL) solution of **1** (2.00 g, 6.50 mmol) were added anhydrous triethylamine (TEA) (2.70 mL, 19.50 mmol) and $Pd(OAc)_2$ (146 mg, 0.65 mmol) under an argon atmosphere. Diphenylphosphine (1.40 mL, 7.80 mmol) was slowly added at room temperature via a syringe with stirring. The resultant solution turned deep red immediately and was heated at reflux until **1** was completely consumed as monitored by TLC analysis. After removal of the solvent, the residue was dissolved in CH_2Cl_2/H_2O (300 mL, 1:1 in v/v). The organic layer was separated and washed with HCl (1 M, 20 mL × 3). Removal of the solvent gave a crude product. Recrystallization from CH_3OH/H_2O (40 mL, 1:1 in v/v) afforded **2** as a yellow solid (1.96 g, 83%). ^1H NMR ($CDCl_3$): δ 3.75 (s, 3H), 7.29−7.34 (m, 10 H), 7.66 (br, 1H), 8.07 (br, 2H). ^{31}P NMR ($CDCl_3$): δ −3.32. These data are the same as those reported in the literature.[42]

Preparation of 4-[5′-(*tert*-Butoxycarbonylamino)pentyl)-1-methyl-2-(diphenylphosphino)terephthalate (3). To a CH_2Cl_2 solution (30 mL) of **2** (1.40 g, 3.80 mmol) were added 4-(*N*,*N*-dimethylamino)pyridine (DMAP) (94 mg, 0.77 mmol) and 1-ethyl-3-(3-dimethylaminopropyl)carbodiimide hydrochloride (EDC·HCl) (1.11 g, 5.80 mmol) at room temperature under argon. After the mixture was stirred for 30 min at room temperature, *N*-(*tert*-butoxylcarbonyl)aminopentanol (1.17 g, 5.80 mmol) was added. The reaction mixture was then stirred at room temperature until **2** was completely consumed as monitored by TLC analysis. After removal of the solvent, the crude product was purified by flash chromatography on silica using hexane/EtOAc (3:1) as eluant to give **3** as a bright yellow solid (1.58 g, 76%). ^1H NMR ($CDCl_3$): δ 1.28 (m, 2H), 1.44 (s, 9H), 1.48 (m, 2H,), 1.62 (m, 2H), 3.12 (m, 2H), δ 3.75 (s, 3H), 4.17 (m, 2H), 4.57 (br, 1H), 7.27−7.35 (m, 10 H), 7.58 (d, J = 3.3 Hz, 1H), 8.02 (d, J = 8.0 Hz, 1H), 8.10 (dd, J = 3.3 and 8.0 Hz, 1H). ^{13}C NMR ($CDCl_3$): δ 23.00, 27.91, 28.24, 29.91, 40.14, 52.16, 64.92, 78.89, 128.39, 128.48, 128.76, 128.94, 130.48, 130.51, 132.81, 133.55, 133.83, 134.89, 136.89, 137.03, 137.66, 140.95, 141.33, 155.79, 165.36, 166.42. ^{31}P NMR ($CDCl_3$): δ −3.79. ESI-MS calcd for $C_{31}H_{37}NO_6P^+$: m/z 550.2 (MH^+); found: 550.2 (MH^+). Anal. Calcd for $C_{31}H_{36}NO_6P$ (**3**) C, 67.75; H, 6.60; N, 2.55. Found: C, 67.70; H, 6.73; N, 2.55.

Preparation of 4-(5′-Aminopentyl)-1-methyl-2-(diphenylphosphino)terephthalate (4). To a CH_2Cl_2 (2 mL) solution of **3** (1.38 g, 2.50 mmol) was slowly added trifluoroacetic acid (TFA) (10.0 mL) via syringe. The reaction mixture was stirred at room temperature until **3** was completely consumed as monitored by

Scheme 1. Synthetic Route to 4-{5′-[1-(Dimethylamino)ethylideneamino)pentyl]}-1-methyl-2-(diphenylphosphino)terephthalate (5)

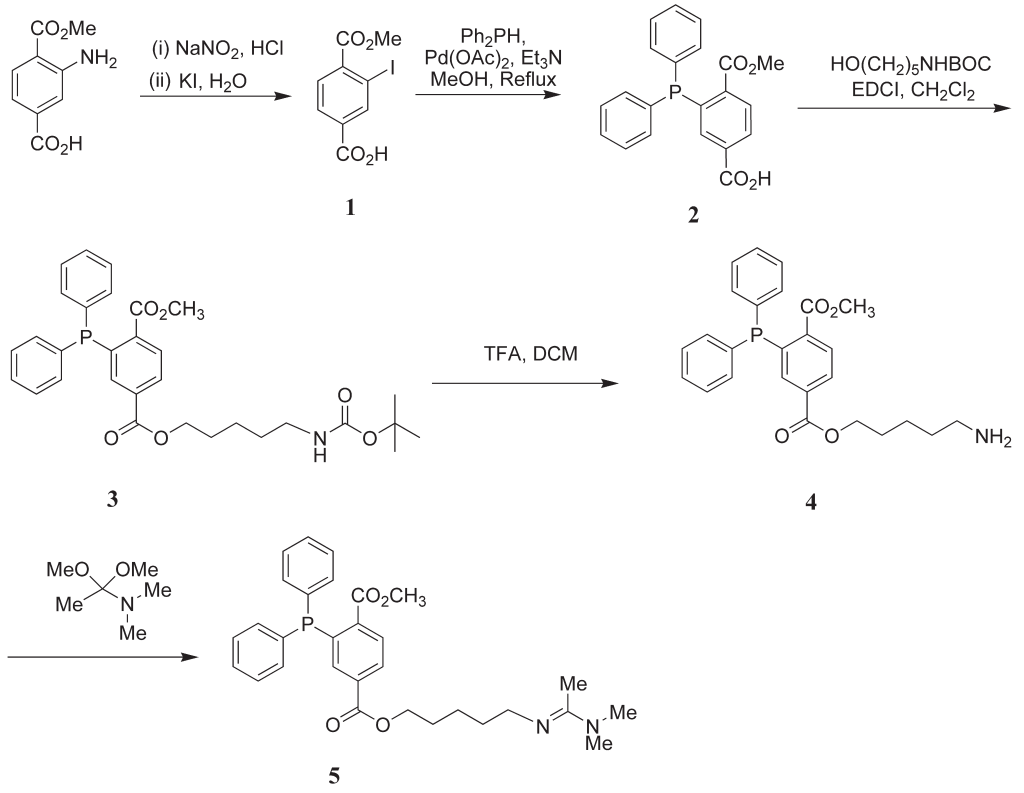

TLC analysis. After removal of the solvent, the residue was redissolved in CH_2Cl_2 (250 mL). The resultant solution was washed with a saturated sodium bicarbonate (50 mL × 3) and saturated sodium chloride solution (50 mL × 3) and dried over anhydrous sodium sulfate. After the removal of the solvent, the crude product was purified by flash chromatography on silica using CH_2Cl_2/CH_3OH (20:1 in v/v) as eluent to give **4** as a viscous yellow liquid (1.05 g, 93%). ^{1}H NMR ($CDCl_3$): δ 1.31 (m, 2H), 1.48 (m, 2H), 1.62 (m, 2H), 2.53 (br, 2H) 2.71 (t, 2H), 3.75 (s, 3H), 4.18 (t, 2H), 7.34 (br, 10 H), 7.61 (d, J = 3.3 Hz, 1H), 8.03 (d, J = 7.9 Hz, 1H), 8.10 (dd, J = 3.3 and 8.0 Hz, 1H). ^{13}C NMR ($CDCl_3$): δ 22.95, 27.95, 32.29, 41.41, 52.06, 64.87, 128.28, 128.38, 128.66, 128.84, 130.37, 130.40, 132.73, 133.46, 133.73, 134.80, 136.82, 136.95, 137.34, 137.60, 140.83, 141.21, 165.27, 166.33. ^{31}P NMR ($CDCl_3$): δ −3.83. MALDI-HRMS calcd for $C_{26}H_{29}NO_4P^+$: m/z 450.1819 (MH^+). Found: 450.1829 (MH^+).

Preparation of 4-{5′-[1-(Dimethylamino)ethylideneamino)-pentyl]}-1-methyl-2-(diphenylphosphino)terephthalate (5). Compound **4** (570 mg, 1.27 mmol) and dimethylacetamide dimethyl acetal (4.0 mL) were stirred under argon at room temperature until a clear solution was formed. The solution was then heated at 60 °C for 1 h. Removal of the volatile chemicals under high vacuum gave **5** as a brown viscous liquid (645 mg, 99%). This product is pure enough for the Staudinger reaction[41] without further purification. As **5** can react with CO_2 in the air, it is necessary to keep it in argon or N_2. The synthetic route to **5** is summarized in Scheme 1. ^{1}H NMR ($CDCl_3$): δ 1.32 (m, 2H), 1.21 (m, 2H,), 1.62 (m, 2H), 1.85 (s, 3H), 2.86 (s, 6H), 3.16 (t, 2H), δ 3.73 (s, 3H), 4.17 (t, 2H), 7.30 (br, 10 H), 7.57 (d, J = 3.3 Hz, 1H), 8.00 (d, J = 7.9 Hz, 1H), 8.07 (dd, J = 3.3 and 8.0 Hz, 1H). ^{13}C NMR ($CDCl_3$): δ 22.96, 27.96, 29.97, 40.69, 41.97, 45.49, 52.23, 64.91, 128.28, 128.48, 128.57, 128.90, 129.00, 130.54, 132.84, 133.60, 133.88, 134.97, 136.90, 137.04, 137.55, 137.80, 140.91, 141.29, 162.15, 165.44, 166.58. ^{31}P NMR ($CDCl_3$): δ −2.73. MALDI-HRMS calcd for $C_{30}H_{36}N_2O_4P^+$: m/z 519.2418 (MH^+). Found: 519.2407 (MH^+).

Preparation of Poly(*p*-chloromethylstyrene)-*co*-polystyrene (PCMS-*co*-PS). A mixture of 2,2,6,6-tetramethylpiperidine-1-oxyl (TEMPO) (52 mg, 0.33 mmol), benzoyl peroxide (BPO) (40 mg, 0.17 mmol), styrene (6.0 mL, 52.4 mmol), *p*-chloromethylstyrene (8.0 mL, 56.2 mmol), and acetic anhydride (60 μL, 0.66 mmol) was degassed by three freeze/thaw cycles, sealed under argon, and heated at 130 °C for 16 h. The polymerization was stopped in liquid nitrogen. The viscous reaction mixture was then dissolved in dichloromethane (50 mL) and precipitated (two times) into methanol (1 L). The precipitate was collected by filtration and dried overnight in a vacuum oven to give PCMS-*co*-PS (12.6 g, 87% yield). THF-GPC: M_n = 3.6 × 10^4 g/mol. PDI = 1.32. The molar ratio of *p*-chloromethylstyrene repeating unit (φ_{CMS}) is 0.56 as measured by NMR.

Preparation of Poly(*p*-azidomethylstyrene)-*co*-polystyrene (PAMS-*co*-PS). Poly(*p*-chloromethylstyrene)-*co*-polystyrene (5.0 g, 21.4 mmol of *p*-chloromethylstyrene repeating unit) was dissolved in DMF/DMSO (90 mL, 1:2 in v/v), to which was added sodium azide (7.0 g, 107.0 mmol). The reaction mixture was stirred at room temperature for 2 days and then precipitated into water. The product was redissolved in dichloromethane and reprecipitated in methanol. The resultant solid was collected by filtration and dried overnight in a vacuum oven for 24 h to give PAMS-*co*-PS (3.7 g, 74%). DMF-GPC: M_n = 56 000. PDI = 1.33. The molar ratio of *p*-azidomethylstyrene repeating unit (φ_{AMS}) is 0.56 as measured by NMR. ^{1}H NMR ($CDCl_3$): δ 1.36, 1.76, 4.22, 6.52, 6.99. The chemical shifts of the benzylic protons were changed from 4.50 ppm in PCMS-*co*-PS to 4.22 ppm in PAMS-*co*-PS, indicating that all chloro groups have been converted to azido units.

Preparation of P("amidine"MS)-*co*-PS (6). The general preparative procedure is shown in Scheme 3. Compound **5** (1.04 g, 2.00 mmol) was dissolved in DMF containing 0.5% H_2O (30 mL). After addition of PAMS-*co*-PS (488 mg, 2.10 mmol of *p*-azidomethyl repeating unit), the reaction mixture was stirred at room temperature until the complete consumption of **5** as

Scheme 2. Synthesis of Poly(*p*-azidomethylstyrene-*co*-poly(styrene)) (PAMS-*co*-PS) (Top) and ^{1}H NMR Spectra of Poly(*p*-chloromethylstyrene)-*co*-poly(styrene) (PCMS-*co*-PS) and PAMS-*co*-PS in $CDCl_3$ (Bottom)

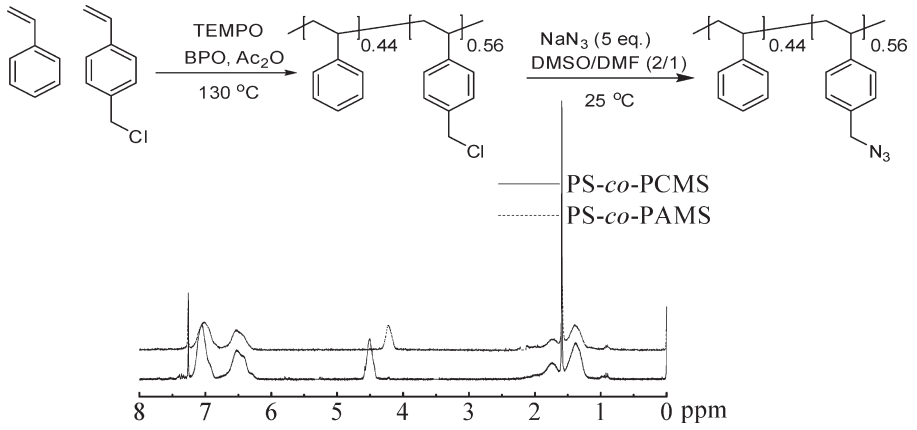

Scheme 3. Synthesis of 6 and ^{31}P NMR Spectra of Both (a) 5 and (b) 6

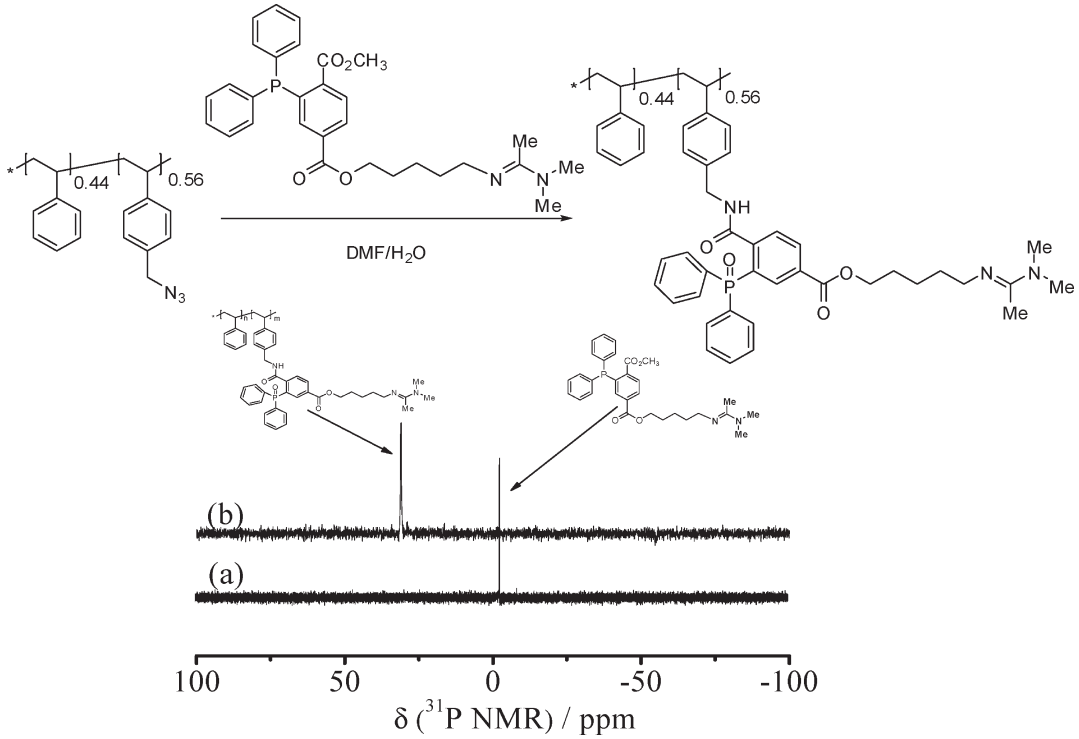

monitored by ^{31}P NMR, in which the ^{31}P chemical shifts were changed from −2.73 ppm in **5** to 30.99 ppm in **6**, as illustrated in Scheme 3. The resultant product poly(4-(4-((5-(1-(dimethylamino)ethylideneamino)pentyloxy)carbonyl)-2-(diphenylphosphoryl)benzoyloxymethylstyrene)-*co*-poly(styrene) (**6**, P("amidine"MS)-*co*-PS) was directly used for LLS studies. DMF/LiBr (50 mM)-GPC: M_n = 112 000. PDI = 1.24, very close to the theoretical value based on the GPC result (M_n) of PCMS-*co*-PS. Note that **6** should be kept in argon or N_2 as it can react with CO_2 in air, and HPLC grade DMF and the deionized water with a resistivity of 18.3 MΩ cm were used in this reaction.

Laser Light Scattering. A commercial LLS spectrometer (ALV/DLS/SLS-5022F) equipped with a multi-τ digital time correlator (ALV5000) and a cylindrical 22 mW He−Ne laser (λ_0 = 632.8 nm, UNIPHASE) as the light source was used. The spectrometer has a high coherence factor of $\beta \sim 0.95$ because of a novel single-mode optical fiber coupled with an efficient avalanche photodiode (APD). The PTFE cap of the LLS scattering cell has four holes. Two of them were connected to a hydrophobic 0.20 μm Millipore Millex-LCR filter and a peristaltic pump. The other two were used for bubbling CO_2 or N_2 gas through a 0.02 μm Whatman filter. The solution of P("amidine"MS)-*co*-PS formed after the ligation in DMF with 0.5% H_2O was clarified by using the filter. The details of LLS instrumentation can be found elsewhere.[46,47]

In dynamic LLS, the intensity−intensity time autocorrelation fuction $G^2(q,t)$, defined as $\langle I(q,0)I(q,t)\rangle/\langle I(q)\rangle^2$, is measured in the homodyne mode, where t is the delay time and $\langle I(q)\rangle$ is the time-average scattering intensity (measured baseline) and q is the scattering vector defined as $4\pi n \sin(\theta/2)/\lambda_0$ with n, θ, and λ_0 the solvent refractive index, the scattering angle, and wavelength in vacuum. $G^2(q,t)$ is related to the normalized electric field−field time correlation function $|g^{(1)}(q,t)|$, defined as $\langle E(q,0)E^*(q,0)\rangle/\langle E(0)E^*(0)\rangle$, by the Siegert relation as[48,49]

$$G^{(2)}(q,t) = A[1+\beta|g^{(1)}(q,t)|^2] \quad \text{or} \quad g^{(2)}(q,t) \equiv \frac{G^{(2)}(q,t)}{A} - 1 = \beta|g^{(1)}(q,t)|^2 \qquad (1)$$

where A is the measured baseline and β is the coherent factor, depending on the detection optics. For a broadly distributed samples or relaxation modes, $|g^{(1)}(q,t)|$ is related to a characteristic relaxation time distribution ($G(\tau)$) as

$$|g^{(1)}(q,t)| = \int_0^\infty G(\tau) \exp(-\frac{t}{\tau})\, d\tau \quad (2)$$

The Laplace inversion of $G^{(2)}(q,t)$ can lead to its corresponding $G(\tau)$. In this study, the CONTIN program in the correlator was used.[50] When $g^{(1)}(q,\tau)$ contains two distinguishable relaxation modes, it can be analyzed using a combination of two exponential functions, i.e.

$$|g^{(1)}(q,t)| = A_f \exp\left(-\frac{t}{\tau_f}\right) + A_s \exp\left(-\frac{t}{\tau_s}\right) \quad (3)$$

where A_f and A_s are intensity contributions of the fast and slow modes, respectively. Note that $A_f + A_s = 1$. In the current study,

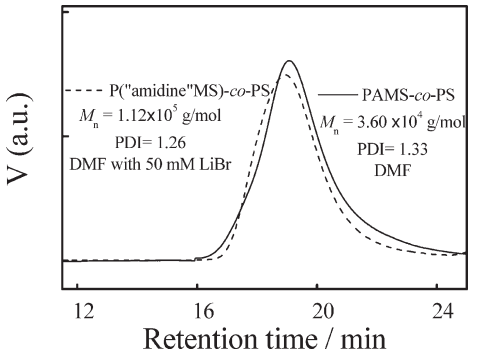

Figure 1. GPC trace obtained for PAMS-*co*-PS and P("amidine"MS)-*co*-PS using DMF and DMF with 50 mM LiBr as eluents.

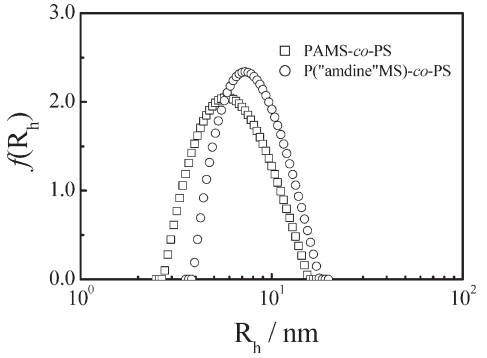

Figure 2. Hydrodynamic radius distributions $f(R_h)$ of PAMS-*co*-PS and PS-*co*-P("amidine"MS) in DMF with 0.5% H_2O.

the solutions temperature was kept at 25 ± 0.05 °C and measured in the angular range 15°−150°.

Results and Discussion

Figure 1 shows that both PAMS-*co*-PS and P("amidine"MS)-*co*-PS are unimodal. On the basis of M_n of starting PAMS-*co*-PS and NMR results, M_n of P("amidine"MS)-*co*-PS should be 1.56×10^5 g/mol, but M_n measured by GPC is 1.12×10^5 g/mol. Such a difference is not surprising because GPC was calibrated by using linear polystyrene standards. Figure 2 further confirms that both PAMS-*co*-PS and P("amidine"MS)-*co*-PS are unimodal, where the two peaks are normalized by the area under each peak. Note that the Staudinger ligation reaction increases the average hydrodynamic radius ($\langle R_h \rangle$, strictly speaking, $\langle R_h \rangle = \langle 1/R_h \rangle^{-1}$) from 5.8 to 7.6 nm, presumably due to large and bulky "amidine" side groups that make the chain less flexible with a more extended conformation. As shown in Scheme 4, alternate bubbling of CO_2 and N_2 through the P("amidine"MS)-*co*-PS solution can make individual chains undergo a neutral−charged−neutral transition.

Figure 3 shows that after CO_2 and N_2 gases were alternatively bubbled 30 min through each solution of P("amidine"MS)-*co*-PS at 25 °C, the solution conductivity measured using a conductivity meter (DDS-307, Shanghai Hongyi Instrumentation, Ltd.) dramatically changes five times and switches between two constant values. The switching is completely reversible. The inset photos in Figure 3 are the appearance of the solution of P("amidine"MS)-*co*-PS in a different solvent (THF) with 0.5% H_2O, in which the charged P("amidine"MS)-*co*-PS chains have an extremely low

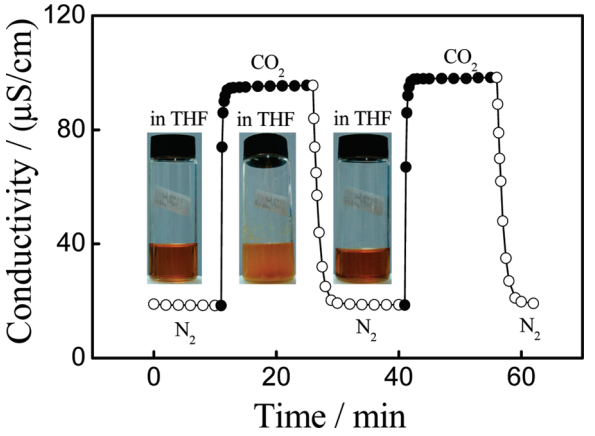

Figure 3. Conductivity of P("amidine"MS)-*co*-PS in DMF with 0.5% H_2O at 25 °C after alternative bubbling of CO_2 and N_2, where polymer concentration is 7.3 mg/mL. Insets are photos of P("amidine"MS)-*co*-PS in THF with 0.5% H_2O in different states before and after CO_2 and N_2 bubbling, where polymer concentration is 25.0 mg/mL.

Scheme 4. Reversible Change between P("amidine"MS)-*co*-PS and Its Charged State in DMF with 0.5% H_2O after Alternating Bubbling of CO_2 and N_2

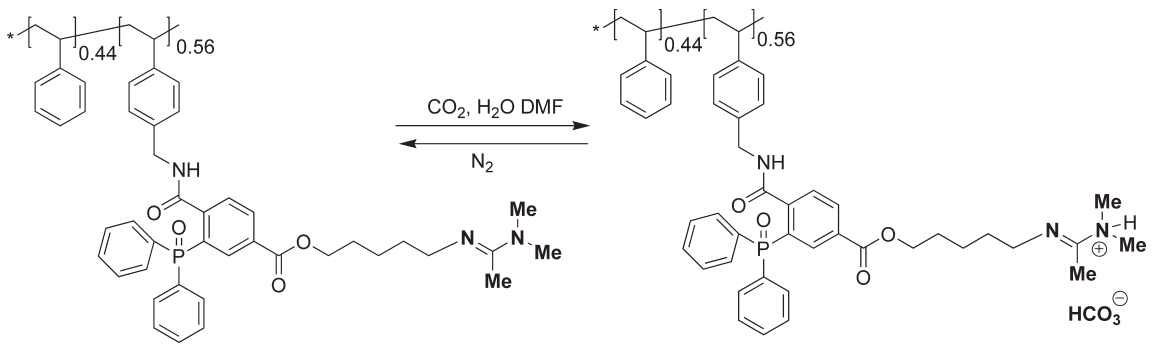

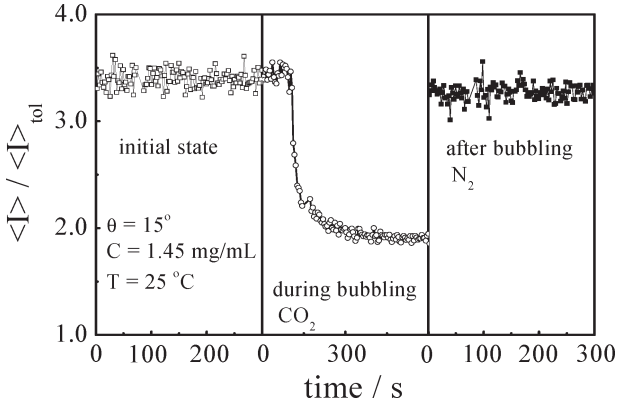

Figure 4. Time dependence of time-average scattering intensity normalized by that of toluene of P("amidine"MS)-*co*-PS in DMF with 0.5% H_2O at different states before and after CO_2 and N_2 bubbling.

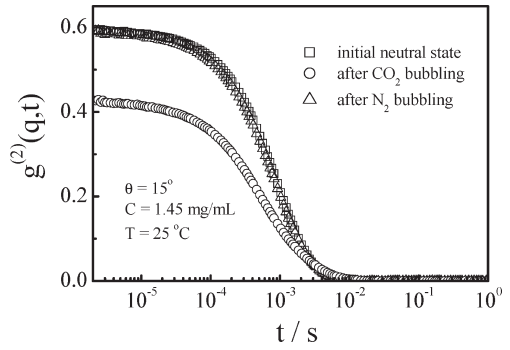

Figure 5. Normalized intensity−intensity time correlation functions in one cycle of CO_2 and N_2 bubbling of P("amidine"MS)-*co*-PS solution.

solubility. The change of solution appearance from clear to cloudy and from cloudy to clear during the alternative bubbling of CO_2 and N_2 clearly shows the neutral-to-charged-to-neutral transition of P("amidine"MS)-*co*-PS chains in THF.

Figure 4 shows that as individual P("amidine"MS)-*co*-PS chains are gradually charged during the CO_2 bubbling, the time average scattering intensity ($\langle I \rangle$) decreases ~45% over a period of ~500 s. The alternative bubbling of CO_2 or N_2 can reversibly switch $\langle I \rangle$ between two average values. Such a decrease of $\langle I \rangle$ in salt-free polyeletrolyte solutions was reported before.[10,23] It has been well-known in LLS that $\langle I \rangle$ is proportional to $(\partial C/\partial \pi)_T$, where C and π are polymer concentration and solution osmotic pressure, respectively. When polymer chains are charged, it is more difficult to induce the concentration fluctuation for a given osmotic pressure change because of electrostatic repulsion. Therefore, such a decrease of $\langle I \rangle$ after the chains are charged is expected.

Figure 5 shows three normalized intensity−intensity time correlation functions ($g^{(2)}(q,t)$) in one cycle of CO_2 and N_2 bubbling of the P("amidine"MS)-*co*-PS solution. After the CO_2 bubbling, the intercept ($\beta_{app} = [g^{(2)}(q,t)]_{t\to 0}$) decreases from 0.59 to 0.42. It is known that $\beta_{app} = \beta[\langle (I - \langle I \rangle)^2 \rangle / \langle I \rangle^2$, where $I = I_{polymer} + I_{solvent}$. As stated before, β is a constant for a given optical setup in a LLS spectrometer. The decrease of β_{app} can be attributed to the decrease of $I_{polymer}$ when the chains are charged in a salt-free solution. The return of β_{app} to 0.59 after the N_2 bubbling also indicates that neutral-to-charged-to-neutral transition is fully reversible.

Figure 6 shows variation of the characteristic relaxation time distribution $G(\tau)$ in one cycle of CO_2 and N_2 bubbling of the P("amidine"MS)-*co*-PS solution. When the chains are their initial neutral state before the CO_2 bubbling, there is only one relaxation

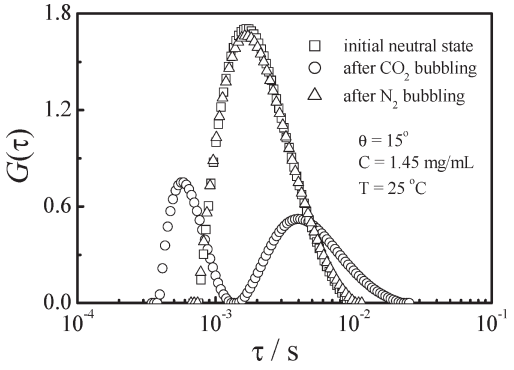

Figure 6. Characteristic relaxation time distributions in one cycle of CO_2 and N_2 bubbling of P("amidine"MS)-*co*-PS solution.

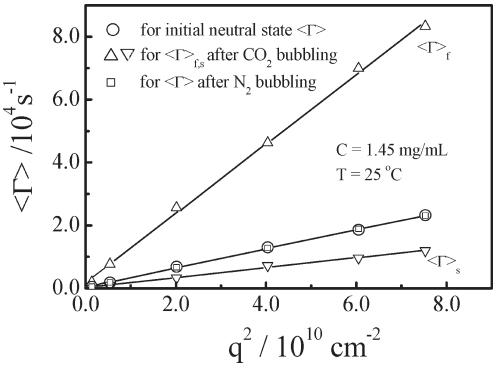

Figure 7. Scattering vector (q) dependence of average characteristic line widths (Γ) in one cycle of CO_2 and N_2 bubbling of P("amidine"MS)-*co*-PS solution.

mode. When each P("amidine"MS)-*co*-PS chain is charged after the CO_2 bubbling, $G(\tau)$ splits into two peaks. The N_2 bubbling can return $G(\tau)$ to its initial state, further indicating that the neutral−charged−neutral transition is completely reversible.

Figure 7 shows that the average characteristic line width ($\langle \Gamma \rangle = 1/\langle \tau \rangle$) is a linear function of the square of the scattering vector (q), passing through the origin, no matter whether the chains are charged, indicating that these relaxation modes are diffusive. As expected, in the initial neutral state, the relaxation is related to translational diffusion. The slope of "$\langle \Gamma \rangle$ vs q^2" leads to a diffusion coefficient $D = 3.6 \times 10^{-7}$ cm^2 s^{-1}, corresponding to $\langle R_h \rangle = 7.6$ nm. After the CO_2 bubbling, each split peak corresponds to one relaxation with one characteristic line width. Both $\langle \Gamma \rangle_{fast}$ and $\langle \Gamma \rangle_{slow}$ are a linear function of q^2, passing through the origin, revealing that they are diffusive with $\langle D \rangle_{fast} = 1.1 \times 10^{-6}$ cm^2 s^{-1} and $\langle D \rangle_{slow} = 1.6 \times 10^{-7}$ cm^2 s^{-1}, corresponding to $\langle R_h \rangle_{fast} = 2.5$ nm and $\langle R_h \rangle_{slow} = 17.8$ nm. As expected, the N_2 bubbling returns "$\langle \Gamma \rangle$ vs q^2" to its initial state. Further, Figure 8 shows that the intensity contribution of the slow relaxation mode (A_s) nearly remains a constant at different scattering angles, where $A_f + A_s = 1$. The q independence of the scattering intensity reveals that the slow mode is not related to some scattering objects larger than $1/q$ (~35−190 nm).

We found that our fast mode agrees well with the interpretation of the coupled diffusion of individual polyelectrolyte chains and their counterions in salt-free dilute solutions proposed by Lin et al.[1,17] and Muthukumar,[18] namely, according to eq 2 in ref 1 and eq 3.25 in ref 18 in the limit condition of $qR_g \ll 1$

$$D_{fast} = \frac{k_B T}{6\pi\eta_0 R_h}\left(1 + N\frac{Z_p{}^2 c}{Z_c{}^2\rho_c + \sum_j Z_j{}^2\rho_j}\right) \qquad (4)$$

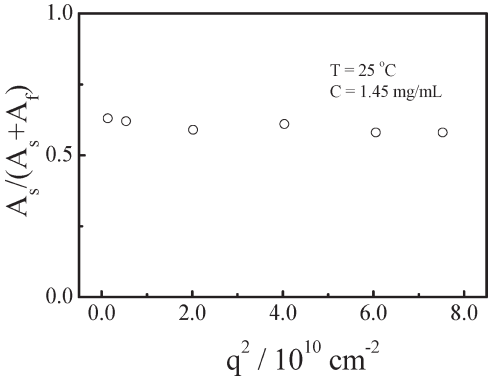

Figure 8. Scattering vector (q) dependence of intensity contribution of slow relaxation mode (A_s) after N_2 bubbling of P("amidine"MS)-*co*-PS solution. Note that $A_s + A_s = 1$.

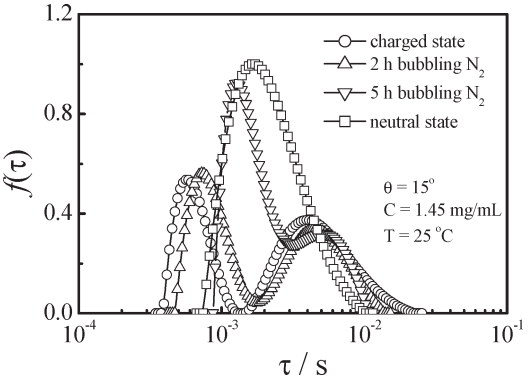

Figure 9. Characteristic relaxation tie distributions $G(\tau)$ during the charged-to-neutral transition induced by slowly bubbling N_2 through P("amidine"MS)-*co*-PS solution.

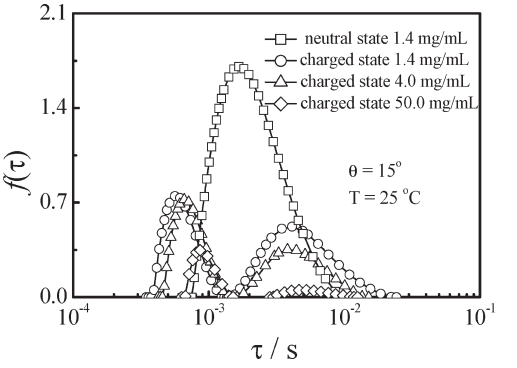

Figure 10. Concentration dependence of characteristic relaxation time distributions $G(\tau)$ of charged P("amidine"MS)-*co*-PS in DMF with 0.5% H_2O.

where R_h is the hydrodynamic radius, η_0 is the solvent viscosity, N is the number of the Kuhn segments, c is the segment concentration, Z_p and Z_c are charges of the segment and counterion, and ρ_c and ρ_j are the number densities of counterions and the jth salt ion, respectively. Note that D_{fast} contains two parts, namely, the diffusion of the center-of-gravity of the chain and an additional coupled term. For neutral polymer chains in a theta solution, their conformation is a random coil and its translational diffusion coefficient (D) is related to R_h as

$$D = \frac{k_B T}{6\pi\eta_0 R_h}$$

and

$$R_h = \frac{3\sqrt{\pi}}{8} R_g = \frac{3\sqrt{\pi}}{8} \frac{lN^{1/2}}{\sqrt{6}} = \frac{\sqrt{3\pi}}{8\sqrt{2}} \frac{Nl}{N^{1/2}} \quad (5)$$

where R_g is the radius of gyration, l is the segment length, and $Nl \sim 70$ nm, the contour length. Since $\langle R_h \rangle \sim 7.6$ nm, we have that $N \sim 6-7$ and $l \sim 10-12$ nm. It is reasonable to have such a long l because of its large "amidine" groups (~3 nm). In the charged state, the chains are even more extended with a rodlike conformation so that its R_h and contour length are related by

$$R_h = \frac{Nl}{2(\ln \alpha - \gamma)} \quad (6)$$

where α is the ratio of the chain length to diameter and $\gamma \simeq 0.3$, a constant related to the chain end effect. Therefore, in the charged state for salt-free dilute solutions and monovalent ions ($\rho_j = 0$, $|Z_p| = |Z_c| = 1$ and $c = \rho_c$)

$$\frac{D_{fast}}{D} = \frac{\sqrt{3\pi}(\ln \alpha - \gamma)}{4\sqrt{2}} \frac{1+N}{N^{1/2}} \quad (7)$$

Here $\alpha \sim 10$ and $N \sim 6-7$ so that $D_{fast}/D = 3.1-3.3$, fairly close to our measured value of 3.27.

Sedlak et al.[11] and Amis et al.[12] also found two relaxation modes and attributed the slow mode to some temporal interchain aggregates. Russo and his co-workers[25] recently concluded that (1) the slow mode is not related to the hydrophobic patches or the centrifugal force or the associated hydrostatic pressure and (2) the residence time of a chain in those temporal aggregates (if exist) is shorter than the fluorescence photobleaching (FPB) recovery time scale (~20 s). On the other hand, for charged colloidal particles in dispersions, Pusey and Tough[51] attributed the fast and slow modes to the mutual and self-diffusion, respectively. Namely, in a short time, each chain moves over a short distance and the diffusion of counterions make the charged particles to diffuse faster. After the relaxation of such "collective diffusion", the "self-diffusion" of individual chains in a long time or over a long length must be retarded by those surrounding interacting particles and becomes detectable in LLS.

In other words, the slow mode is related to the structural relaxation or the correlation length of interacted chains (a cage). For the solution used in Figures 5−7, we found that the slow mode is related to some scattering objects with a dimension similar to the interchain distance (~20 nm), further supporting the cage model. Previously, a similar idea was used to explain the slow mode in a moderate semidilute neutral polymer solution ($C^* < C < C_e$), where C^* and C_e are the overlapping and entanglement concentrations, respectively, as schematically shown in Figure 24 of ref 33. It is appealing to use this model to explain our current results; i.e., the fast mode is attributed to the coupled diffusion between counterions and chains, while the slow mode is related to the self-diffusion of the center-of-mass of individual chains under long-range electrostatic interaction-induced constrains of other surrounding chains, just like a cage, because our results reveal that the slow mode is related to small but slowly moving subjects. Such a cage could also be viewed as temporal aggregates.

Figure 9 shows how $G(\tau)$ changes in the backing charged-to-neutral process when N_2 is bubbled through the solution. The reason to study the charged−neutral process is because the neutral-to-charged transition is too fast to be precisely followed by dynamic LLS. It is clear that during the charged-to-neutral transition, $\langle \tau \rangle_{fast}$ increases, i.e., D_{fast} decreases (the coupled fast relaxation slows down). At the same time, the total scattering intensity $\langle I \rangle$ and the contribution from the slow relaxation (A_s) increase because the chains are less constrained by the electro-

static interaction. The peaks of the fast and slow mode gradually merge together and back to its initial neutral state with one single relaxation mode. The explanation on the basis of eq 4 is as follows. When each chain becomes less charged during the N_2 bubbling, Z_p decreases with its average value less than one and finally approaches zero, but Z_c remains monovalent, according to their definitions; and at the same time, R_h also decreases because of the change of the chain conformation from rodlike to random coil. This is why both D_{fast} and D_{slow} approach D. The increases of $\langle I \rangle$ and A_s are expected because neutral chains scatter more light than charged ones and the coupled diffusive relaxation diminishes when each chain becomes neutral so that A_s increases.

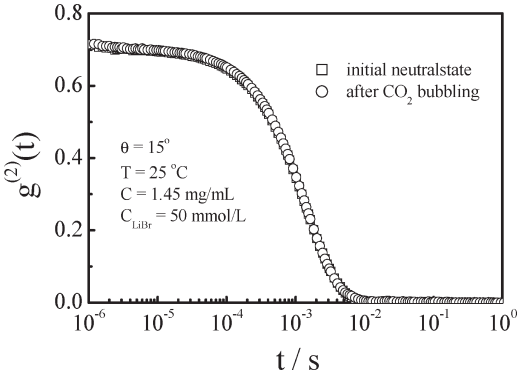

Figure 11. Normalized intensity−intensity time correlation functions of P("amidine"MS)-*co*-PS solution in the presence of 50 mM LiBr before and after CO_2 bubbling.

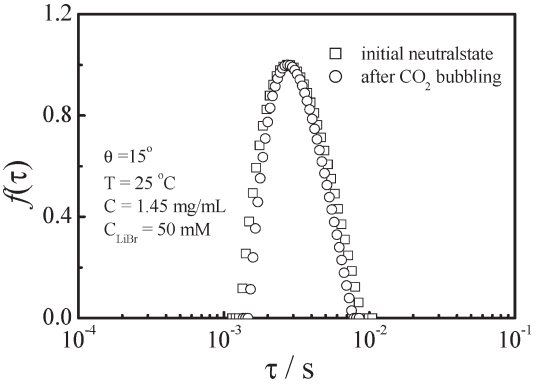

Figure 12. Characteristic relaxation time distributions $G(\tau)$ of P("amidine"MS)-*co*-PS solution in the presence of 50 mM LiBr before and after CO_2 bubbling.

Further, we studied the effect of polymer concentration (C) on dynamics of salt-free dilute polyelectrolyte solutions. Figure 10 shows how $G(\tau)$ varies with C for the charged chains. For comparison, we have normalized the total area under each $G(\tau)$ by its corresponding total scattering intensity and polymer concentration, where we have taken the peak area of $G(\tau)$ in the neutral state as 100%. Note that C^*, defined as $M/(4\pi R_g^3 N_A/3)$ or $M/[(2R_g)^3 N_A]$, is in the range 17−30 mg/mL. Therefore, our polymer concentrations used covers both the dilute and semi-dilute regions. It is clear that $\langle \tau \rangle_{fast}$ increases, i.e., D_{fast} decreases, with C, but $\langle \tau \rangle_{slow}$ (or D_{slow}) nearly remains; and at the same time, both $\langle I \rangle / C$ and A_s decrease. These results are different from the prediction; namely, $D_{fast} \sim C^0$ (eq 3.55b in ref 18). The exact reason is still unknown, but a reasonable speculation is as follows. The increase of polymer concentration gradually screens out the electrostatic interaction, and the effective charges on each chain is less, which has a similar effect as the N_2 bubbling, as shown in Figure 9.

On the other hand, if the slow mode was related to large ion-cloud-overlapping-induced temporal chain aggregates, we would see that the dilution increases $\langle \tau \rangle_{slow}$ because there is less ion-cloud overlapping or, in other words, those temporal aggregates would be smaller. However, Figure 10 shows an opposite trend. The explanation might be as follows. Polymer chains contracted as the concentration increases, resulting in a faster self-diffusion, and at the same time, the interchain friction increases, retarding the self-diffusion in a long time scale. Therefore, increasing the polymer concentration has two opposite effects on the slow mode.

We also studied the effect of salt on dynamics of dilute polyelectrolyte solutions. Figures 11 and 12 show that in the presence of 50 mM LiBr the CO_2 bubbling has no effect on $g^{(2)}(q,t)$ of charged P("amidine"MS)-*co*-PS chains in dilute solutions and its corresponding $G(\tau)$; namely, the addition of 50 mM

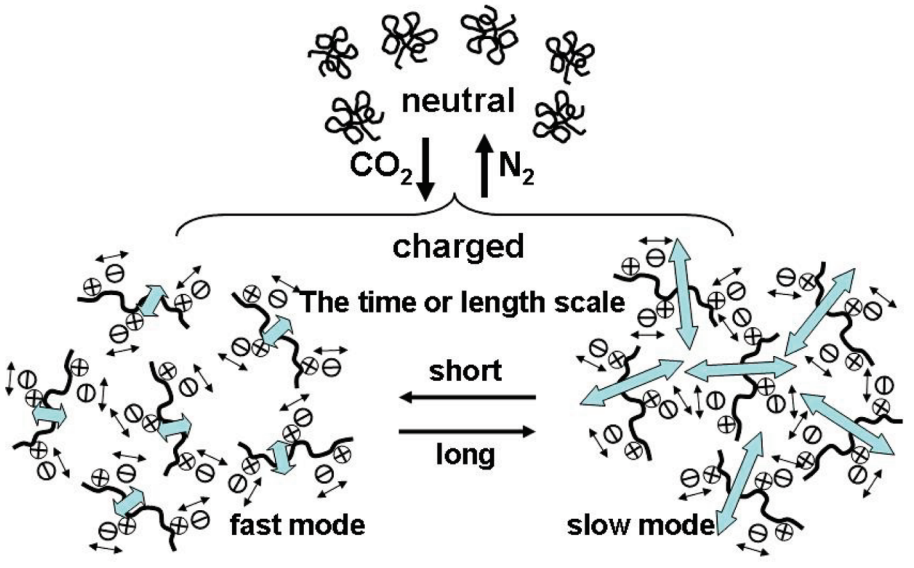

Figure 13. Schematic of fast and slow relaxation modes after each P("amidine"MS)-*co*-PS chain becomes charged after the CO_2 bubbling; namely, the fast mode is due to the coupling of the diffusion of the chain and the wiggling of chain segments induced by fluctuation of counterions condensed nearby the charged chain backbone in a salt-free or low-salt solution and the slow mode to the self-diffusion of the charged chain with an extended conformation.

LiBr sufficiently suppress electrostatic interaction among charges on the chain backbone so the charged chains behave like in the initial neutral state with $\langle D \rangle = 2.33 \times 10^{-7}$ cm^2 s^{-1} and $\langle R_h \rangle =$ 10.0 nm. It should be stated that there is also no change in the time-average scattering intensity. Using eq 4, we can explain these results as follows. The second term in the bracket of eq 4 diminishes because ρ_j is much higher than ρ_c. The screening of electrostatic interaction among different chains also reduces the interchain interaction. Therefore, both D_{fast} and D_{slow} approach D. The slightly larger $\langle R_h \rangle$ is attributed to the chain swelling because the addition of LiBr makes DMF a better solvent.

Conclusion

By designing, synthesizing, and using a novel P("amidine"MS)-*co*-PS that can be *in situ* and reversibly switched between a neutral to a charged state by alternative bubbling of CO_2 and N_2, we have re-examined dynamics of polyelectrolyte solutions by laser light scattering. The current experiments decisively rule out any possible contamination introduced during the solution preparation or the hydrophobic patch-induced interchain aggregation. Our results reconfirm that when individual polymer chains are charged in salt-free dilute solutions, their translational diffusive relaxation in the neutral state splits into a fast and a slow diffusive mode (D_{fast} and D_{slow}), respectively, due to the long-range electrostatic interaction. As expected, adding 50 mM LiBr can suppress the electrostatic interaction so that the charged chains behave like the neutral ones with only one translational diffusive relaxation mode. Further, we found that as the concentration increases, the fast coupled diffusion slows down and the slow self-diffusion is less affected, presumably due to a balance between the screening of the electrostatic interaction and the increase of interchain friction. The fast mode can be attributed to the coupled diffusion originated from a convective current generated by an induced electric field arising from fluctuation of all charged species (charges on the chain and counterions) in the solution in a short time or length scale. Although there is still no decisive evidence to differentiate whether the slow relaxation is related to large temporal aggregates formed due to the overlapping of ion clouds among different chains or to the self-diffusion of individual chains retarded by surrounding chains (interchain friction) in a long time or length scale. Our results indicate that the slow mode is not related to large but slowly moving scattering objects, supporting the assumption of the retarded self-diffusion, as schematically shown in Figure 13. Note that a cage could be viewed as a temporal aggregate.

Acknowledgment. This work was supported by the Ministry of Science and Technology of China (2007CB936401), the National Natural Science Foundation of China (50773077), and the Hong Kong Special Administration Region Earmarked Grant (CUHK4037/07P, 2160331). Junfang is grateful to the China Postdoctoral Science Foundation (No. 20070420727), and Z.K. thanks the Croucher Foundation for his postgraduate studentship. We also thank Prof. M. Muthukumar from UMass and Y. Tang from SIOC for some helpful discussions.

References and Notes

(1) Lin, S. C.; Lee, W. I.; Schurr, J. M. *Biopolymers* **1978**, *17*, 1041.
(2) Schmitz, K. S.; Lu, M.; Gauntt, J. *J. Chem. Phys.* **1983**, *78*, 5059.
(3) Mathiez, P.; Mouttet, C.; Weisbuch, G. *Biopolymers* **1981**, *20*, 2381.
(4) Drifford, M.; Dalbiez, J. P. *Biopolymers* **1985**, *24*, 1501.
(5) Borsali, R.; Nguyen, H.; Pecora, R. *Macromolecules* **1998**, *31*, 1548.
(6) Koene, R. S.; Mandel, M. *Macromolecules* **1983**, *16*, 973.
(7) Sedlák, M.; Konák, C.; Stepánek, P.; Jakes, J. *Polymer* **1987**, *28*, 873.
(8) Schmitz, K. S.; Yu, J. *Macromolecules* **1988**, *21*, 484.
(9) Mattoussi, M.; Karasz, F. E.; Langley, K. H. *J. Chem. Phys.* **1990**, *93*, 3593.
(10) Förster, S.; Schmidt, M.; Antonietti, M. *Polymer* **1990**, *31*, 781.
(11) Sedlák, M.; Amis, E. J. *J. Chem. Phys.* **1992**, *96*, 817.
(12) Ermi, B. D.; Amis, E. J. *Macromolecules* **1996**, *29*, 2701; **1998**, *31*, 7378.
(13) Topp, A.; Belkoura, L.; Woermann, D. *Macromolecules* **1996**, *29*, 5392.
(14) Nerling, W.; Nordmeir, E. *Polym. J.* **1997**, *29*, 795.
(15) Valachovic, D. E.; Amis, E. J.; Tomalia, D. A. *ACS Polym. Prepr.* **1995**, *36*, 373.
(16) Dobrynina, A. V.; Rubinstein, M. *Prog. Polym. Sci.* **2005**, *30*, 1049.
(17) Lee, W. I.; Schurr, J. M. *Chem. Phys. Lett.* **1973**, *23*, 603.
(18) Muthukumar, M. *J. Chem. Phys.* **1996**, *105*, 5183; **1997**, *107*, 2619; *Adv. Chem. Phys.* **2005**, *131*, 1.
(19) Li, X.; Reed, W. F. *J. Chem. Phys.* **1991**, *94*, 4568.
(20) Reed, W. F.; Ghosh, S.; Medjahdi, G.; Francois, J. *Macromolecules* **1991**, *24*, 6189.
(21) Ghosh, S.; Li, X.; Reed, C. E.; Reed, W. F. *Biopolymers* **1991**, *30*, 1101.
(22) Peitzsch, R. M.; Burt, M. J.; Reed, W. F. *Macromolecules* **1992**, *25*, 806.
(23) Ghosh, S.; Peitzsch, R. M.; Reed, W. F. *Biopolymers* **1992**, *32*, 1105.
(24) Ermi, B. D.; Amis, E. J. *Macromolecules* **1998**, *31*, 7378.
(25) Cong, R.; Temyanko, E.; Russo, P. S.; Edwin, N.; Uppu, R. M. *Macromolecules* **2006**, *39*, 731.
(26) Kirkwood, J. G.; Shumaker, J. B. *Proc. Natl. Acad. Sci. U.S.A.* **1952**, *38*, 855.
(27) Oosawa, F. *Biopolymers* **1968**, *6*, 1633.
(28) Ise, N.; Okubo, T.; Hiragi, Y.; Yamamoto, K.; Kawai, H.; Hashimoto, T.; Fujimura, M.; Nakajima, A.; Hayashi, H. *J. Am. Chem. Soc.* **1980**, *102*, 7901. Sogami, I.; Ise, N. *J. Chem. Phys.* **1984**, *81*, 6320.
(29) Schmitz, K. S.; Parthasarathy, N.; Vottler, E. *Chem. Phys.* **1982**, *66*, 187. Schmitz, K. S.; Lu, M.; Gauntt, J. *J. Chem. Phys.* **1983**, *78*, 5059. Schmitz, K. S.; Ramsay, D. J. *Biopolymers* **1985**, *24*, 1247. Ramsay, D. J.; Schmitz, K. S. *Macromolecules* **1985**, *18*, 2422. Schmitz, K. S. *Phys. Rev. E* **2002**, *66*, 061403.
(30) Ngai, T.; Wu, C. *Macromolecules* **2003**, *36*, 848.
(31) Ngai, T.; Wu, C.; Chen, Y. *J. Phys. Chem. B* **2004**, *108*, 5532.
(32) Ngai, T.; Wu, C.; Chen, Y. *Macromolecules* **2004**, *37*, 987.
(33) Li, J.; Li, W.; Huo, H.; Luo, S.; Wu, C. *Macromolecules* **2008**, *41*, 901.
(34) Jessop, P. G.; Heldebrant, D. J.; Li, X.; Eckert, C. A.; Liotta, C. L. *Nature* **2005**, *436*, 1102.
(35) Liu, Y.; Jessop, P. G.; Cunningham, M.; Eckert, C. A.; Liotta, C. L. *Science* **2006**, *313*, 958.
(36) Goto, A.; Hawker, C. J. *Acc. Chem. Res.* **1997**, *30*, 373.
(37) Moad, G.; Fukuda, T. *Macromolecules* **1997**, *30*, 4272.
(38) Hawker, C. J.; Elce, E.; Dao, J.; Volksen, W.; Russell, T. P.; Barclay, G. P. *Macromolecules* **1996**, *29*, 2686.
(39) Rizzardo, E. *Macromolecules* **1995**, *28*, 8722.
(40) Kohn, M.; Breinbauer, R. *Angew. Chem., Int. Ed.* **2004**, *43*, 3106.
(41) Saxon, E.; Bertozzi, C. R. *Science* **2000**, *287*, 2007.
(42) Kiick, K. L.; Saxon, E.; Tirrell, D. A.; Bertozzi, C. R. *Proc. Natl. Acad. Sci. U.S.A.* **2002**, *99*, 19.
(43) Lin, F. L.; Hoyt, H. M.; van Halbeek, H.; Bergman, R. G.; Bertozzi, C. R. *J. Am. Chem. Soc.* **2005**, *127*, 2686.
(44) Mattingly, P. G. *Synthesis* **1990**, 366.
(45) Bredereck, H.; Effenberger, F.; Simchen, G. *Angew. Chem.* **1961**, *73*, 493.
(46) Chu, B. *Laser Scattering*, 2nd ed.; Academic Press: New York, 1991.
(47) Wu, C.; Zhou, S. Q. *Macromolecules* **1995**, *28*, 8381.
(48) Berne, B.; Pecroa, R. *Dynamic Light Scattering*; Plenum Press: New York, 1976.
(49) Bwown, W. *Light Scattering: Principles and Development*; Clarendon Press: Oxford, U.K., 1996.
(50) Provencher, S. W. *J. Chem. Phys.* **1978**, *69*, 4273.
(51) Pusey, P. N.; Tough, R. J. A. *Adv. Colloid Interface Sci.* **1982**, *16*, 143.